Osmium Recycling in Subduction Zones

Alan D. Brandon,* Robert A. Creaser, Steven B. Shirey,
Richard W. Carlson

Peridotite xenoliths from the Cascade arc in the United States and in the Japan arc have neodymium and osmium isotopic compositions that are consistent with addition of 5 to 15 percent of subducted material to the present-day depleted mantle. These observations suggest that osmium can be partitioned into oxidized and chlorine-rich slab-derived fluids or melts. These results place new constraints on the behavior of osmium (and possibly other platinum group elements) during subduction of oceanic crust by showing that osmium can be transported into the mantle wedge.

Studies of the isotopic compositions and large-ion lithophile and light element abundances of arc lavas (*1–3*) have shown the importance of recycled subducted material in the genesis of arc magmas. Possible slab-derived melts have also been identified in arc peridotite xenoliths (*4*). Osmium isotopic studies provide a useful way to view the process of crustal recycling, because Re/Os ratios in the oceanic lithosphere are up to several orders of magnitude higher than in mantle peridotite, and Re and Os both display chalcophile and siderophile behavior (*5–12*). Decay of ^{187}Re [$\lambda = 1.64 \times 10^{-11}$ years^{-1} (*13*)] to ^{187}Os in oceanic crust in just tens of millions of years will produce an ^{187}Os/^{188}Os ratio up to an order of magnitude higher than that in the present-day mantle. This radiogenic Os potentially could elevate ^{187}Os/^{188}Os ratios in the mantle above subduction zones. Many ocean island basalts have ^{187}Os/^{188}Os ratios that are higher than chondritic ^{187}Os/^{188}Os ratios, and these have been explained by recycling of ocean crust into the deep mantle source regions of ocean island volcanism (*12*). To further understand the role of subducted slabs in volcanic arc magma genesis and the geochemical cycle of Re and Os at convergent margins, we analyzed Os and Nd isotopic compositions in spinel peridotite xenoliths from lavas erupted in the Plio-Pleistocene from Ichinomegata, Japan (*14*), and Simcoe, Washington [Cascades (*15*, *16*)], both of which sample the wedge mantle because they are located about 50 km to the back-arc side of present-day volcanic arc fronts. Because of very low abundances of Os in arc basalts [typically <10 parts per thousand (ppt)], direct analysis of arc lavas has been difficult and has yielded ambiguous results.

The peridotite xenoliths chosen for study are fresh, with no signs of visible alteration. The Simcoe samples are Cr-diopside–bearing spinel harzburgites with high Mg numbers [molar Mg/(Mg + Fe^{2+}) of 0.910 to 0.914] and major element compositions indicative of extraction of a melt (*16*). They contain rare phlogopite (*15*, *16*) and subchondritic Sm/Nd ratios indicative of elevated light rare earth element abundances relative to melt-depleted mantle. These features are interpreted as arising from later metasomatic processes. The Ichinomegata samples are Cr-diopside–bearing spinel lherzolites with Mg numbers from 0.89 to 0.91, which are typical of depleted-to-fertile mantle (*14*). These samples have Sm/Nd ratios ranging from chondritic to higher than chondritic (light rare earth element depletion, Table 1) that are similar to ratios in abyssal peridotites (*17*), which are interpreted to result in part from melt removal. The presence of pargasite in some of these samples, as well as Sr-Nd isotopic compositions extending from the depleted mantle field to higher ^{87}Sr/^{86}Sr and lower ^{143}Nd/^{144}Nd ratios (*18*), reflect metasomatic events after melt depletion. The xenoliths from both locales have high oxygen fugacities [about 0.5 to 1.5 log units greater than that of the fayalite-magnetite-quartz buffer (*19*, *20*)] relative to those of modern mantle samples not directly associated with volcanic arcs. This feature is consistent with the peridotites having interacted with water-bearing fluids or magmas derived from subducting slabs (*20*, *21*).

Several of the xenoliths have ^{187}Os/^{188}Os ratios of 0.1277 to 0.1338. These values are higher than ratios for present-day depleted mantle [0.1220 to 0.1270 (*9*)] or chondritic mantle [^{187}Os/^{188}Os = 0.1275 (Table 1 and Fig. 1)]. Subcontinental mantle peridotites, massif peridotites, and abyssal peridotites typically have near-chondritic to strongly subchondritic ^{187}Os/^{188}Os ratios, reflecting Os retention and Re removal during partial melting (*5–7*, *9*, *10*). Most Simcoe and Ichinomegata xenoliths have subchondritic ^{187}Re/^{188}Os ratios and were erupted less than 1 million years ago (Ma), so the ^{187}Os/^{188}Os values above chondritic values cannot be accounted for by in situ ^{187}Re decay. These high ^{187}Os/^{188}Os ratios may instead represent addition of radiogenic Os to these samples after some melt was extracted from these parts of the mantle.

The Sm-Nd isotopic data for the Ichinomegata samples plot as an array from ^{143}Nd/^{144}Nd of 0.51335 to 0.51280, and from ^{147}Sm/^{144}Nd of 0.38 to ~0.2 (Fig. 2). Such an array can be interpreted as either an isochron or a mixing line between two components. If this array was the result of variable degrees of depletion from a fertile mantle, then an isochron of 400 Ma ap-

Table 1. Bulk rock Al_2O_3 (weight %), Sm-Nd isotopic systematics of clinopyroxene separates, and Re-Os isotopic systematics of bulk rock samples of the Simcoe (Sim) harzburgite and Ichinomegata (I) lherzolite xenoliths are shown (*29*). Alumina data for Simcoe are x-ray fluorescence (XRF) analyses (*20*). All data for Ichinomegata are XRF analyses, except for I-102, which is an inductively coupled plasma analysis. Dashes indicate not analyzed for.

Sample	Al_2O_3	Sm (ppm)	Nd (ppm)	^{147}Sm/^{144}Nd	^{143}Nd/^{144}Nd	Re (ppt)	Os (ppt)	^{187}Re/^{188}Os	^{187}Os/^{188}Os
		Clinopyroxene				Bulk rock			
Sim-1	–	0.988	4.52	0.1322	0.513042	–	–	–	–
Sim-2	1.30	0.810	5.74	0.0854	0.512994	37.4	322	0.547	0.1278*
Sim-3	1.05	0.384	1.86	0.1249	0.512920	52.2	671	0.366	0.1304
Sim-9c	1.45	2.57	12.92	0.1203	0.512990	56.9	743	0.360	0.1244
Sim-12	1.27	2.62	13.88	0.1142	0.512893	38.9	479	0.382	0.1277*
Sim-24	1.32	0.325	1.21	0.1625	0.512928	–	1374	–	0.1285*
						14.7	1056	0.066	0.1287*
I-6	3.16	1.41	2.58	0.3306	0.513197	24.8	420	0.285	0.1206
I-9	3.60	1.53	2.56	0.3616	0.513046	63.8	2080	0.144	0.1329*
I-10	3.01	1.18	2.16	0.3305	0.513197	82.9	304	1.284	0.1265
I-11	2.72	0.519	1.01	0.3109	0.513059	71.0	1756	0.190	0.1259*
I-12	3.07	1.31	2.07	0.3829	0.513258	25.4	624	0.196	0.1227
I-101	–	0.338	0.994	0.2057	0.512822	9.3	123	0.365	0.1338
I-102	2.62	1.02	1.82	0.3390	0.513213	108.2	954	0.547	0.1228

*Re-Os data were obtained at DTM; all other Re-Os data were obtained at the University of Alberta.

A. D. Brandon, S. B. Shirey, R. W. Carlson, Department of Terrestrial Magnetism, Carnegie Institution of Washington, 5241 Broad Branch Road, NW, Washington, DC, USA, 20015.
R. A. Creaser, Department of Earth and Atmospheric Sciences, University of Alberta, 126 Earth Sciences Building, Edmonton, Alberta, Canada T6G 2E3.

*To whom correspondence should be addressed.

proximates the time of depletion of these peridotites (Fig. 2). Combined Re-Os and Sm-Nd isotopic systematics are not consistent with this interpretation. The Ichinomegata samples with $^{187}Os/^{188}Os$ ratios that are higher than chondritic $^{187}Os/^{188}Os$ ratios (samples I-9 and I-101, Table 1) have subchondritic Re/Os ratios and hence give negative model depletion ages, which is inconsistent with long-term decay of ^{187}Re after melt depletion in a closed system. These samples also have the lowest $^{143}Nd/^{144}Nd$ ratios (Table 1 and Fig. 3), and this coupling instead is more likely to result from mixing of depleted mantle with an isotopic component with low $^{143}Nd/^{144}Nd$ and high $^{187}Os/^{188}Os$ ratios.

For the Simcoe samples, their subchondritic $^{147}Sm/^{144}Nd$ ratios (elevated light rare earth element abundances), lack of correlation between Sm and Nd isotopic data (Fig. 2), and similarity of $^{143}Nd/^{144}Nd$ and $^{87}Sr/^{86}Sr$ compositions with those of Pliocene Simcoe lavas (*16, 22*) are consistent with recent addition of isotopically distinct Nd and Sr to depleted mantle.

The combined Nd and Os isotopic data for Simcoe and Ichinomegata samples indicate mixing between isotopically distinct Os components. Lower $^{187}Os/^{188}Os$ ratios are coupled with higher $^{143}Nd/^{144}Nd$ ratios that form a band extending from typical depleted mantle values to those with higher $^{187}Os/^{188}Os$ ratios and lower $^{143}Nd/^{144}Nd$ ratios (Fig. 3). This negative correlation between Nd and Os isotopic compositions is not evident in data for cratonic mantle xenoliths (*6, 7*), abyssal peridotites (*5, 9, 10*), or peridotite massifs (*5, 23*).

Correlation between $^{187}Os/^{188}Os$ ratios and Al_2O_3 concentrations provides further support for the idea that these samples represent mixing between depleted mantle and radiogenic Os components (Fig. 4). Some peridotite massifs with high Al_2O_3 concentrations indicative of little melt extraction have near-chondritic present-day $^{187}Os/^{188}Os$ ratios, whereas more depleted peridotites have low $^{187}Os/^{188}Os$ ratios, reflecting removal of Re and Al_2O_3 during melting (*23*). Samples from individual massifs commonly plot on lines that reflect ages and degrees of melting (*23*). The samples from Simcoe and Ichinomegata do not show such characteristics, but instead plot as oblique arrays, indicating mixing between depleted mantle and a source with abundant radiogenic Os.

Mixing models can be used to evaluate the effects of metasomatism of mantle by fluids or melts for Nd and Os derived from subducting slabs (*24*). The Simcoe data can be produced by mixing about 7 to 15% by mass of a subduction component containing 90 to 95% subducted basalt and 5

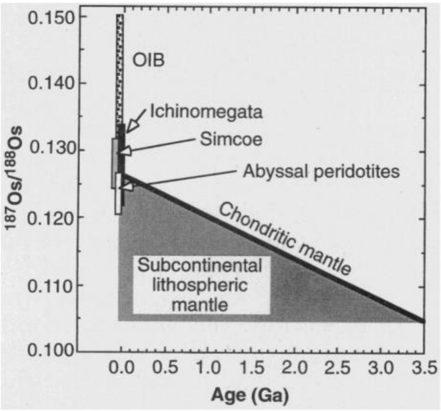

Fig. 1. Os isotopic evolution diagram [data sources were (*5–7*) and (*9–12*)]. Oceanic island basalts (OIB) are samples considered not to have been contaminated by oceanic lithosphere material (*12*). The abyssal peridotite range is as defined by Snow and Reisberg (*9*). Both Simcoe and Ichinomegata have $^{187}Os/^{188}Os$ ratios that are higher than chondritic $^{187}Os/^{188}Os$ ratios in some samples, unlike reported subcontinental lithospheric mantle from other locales not associated with present-day subduction. Ga, billions of years ago.

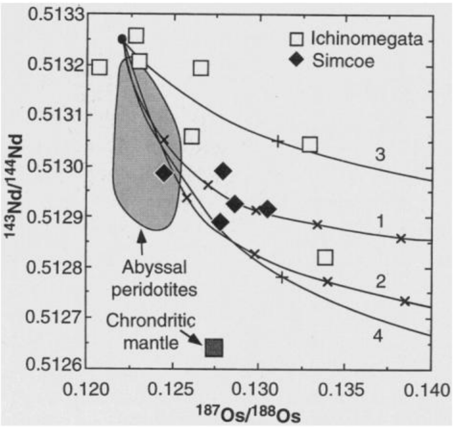

Fig. 3. Nd-Os isotopic relations for the Simcoe and Ichinomegata samples. Mixing curves (*24*) are as follows: 1: Juan de Fuca, $95_{bas}:5_{sed}$; 3:1 mix ratio [denotes Juan de Fuca slab (under the Cascades) with the subduction component calculated as 95% basalt (bas) and 5% sediment (sed), with an Os mantle peridotite-to-subduction component abundance mixing ratio of 3:1. 2: Juan de Fuca, $90_{bas}:10_{sed}$; 2.5:1 mix ratio. 3: Pacific, $95_{bas}:5_{sed}$; 4:1 mix ratio ("Pacific" denotes the Pacific slab under Japan). 4: Pacific, $80_{bas}:20_{sed}$; 4:1 mix ratio. Crosses on the mixing curves indicate the percentages of the subduction component added to peridotite in the mix, in 5% increments. The $^{187}Os/^{188}Os$ subduction components for mixtures 1, 2, 3, and 4 are 0.2620, 0.3020, 0.8859, and 0.8400, respectively, and are calculated as previously described (*24*). Abyssal peridotite data are from Snow and co-workers (*9, 24*).

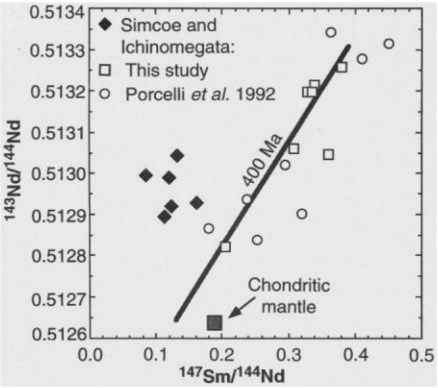

Fig. 2. Sm-Nd isotopic systematics of clinopyroxenes from Simcoe and Ichinomegata peridotites. Additional published data on Ichinomegata samples are plotted as circles (*18*). A reference line of 400 Ma is plotted for six of seven Ichinomegata samples analyzed in this study.

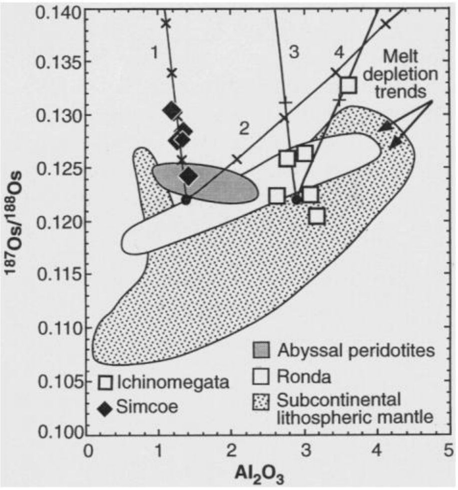

Fig. 4. Os-Al_2O_3 relations for the Simcoe and Ichinomegata samples. A melt depletion trend is recorded by the Ronda peridotite data (*23*). Subcontinental lithospheric mantle data are from harzburgite and lherzolite xenoliths from the United States, China, Mexico, Australia, and Kaapvaal (southern Africa) cratons (*6, 30*). Abyssal peridotite data are from Snow and co-workers (*9, 30*). Mixing curves are for a depleted mantle with $^{187}Os/^{188}Os = 0.122$ (to conform with the Os mixing models in Fig. 3) and with Al_2O_3 for Simcoe and Ichinomegata mixing curves equal to 1.4 weight % and 2.9%, respectively, which are mixed with subduction components (Os is as defined in Fig. 3), with Al_2O_3 equal to 0 and 15%. The former is considered to be a hydrous fluid and the latter a melt. The Simcoe data correspond to the 0% Al_2O_3 mixing curve, whereas Ichinomegata lies between the 0 and 15% mixing curves. Crosses on the mixing curves are as in Fig. 3, in 5% increments. Mixing curves are as follows: 1: Juan de Fuca, $90_{bas}:10_{sed}$; 0% Al_2O_3. 2: Juan de Fuca, $90_{bas}:10_{sed}$; 15% Al_2O_3. 3: Pacific, $80_{bas}:20_{sed}$; 0% Al_2O_3. 4: Pacific, $80_{bas}:20_{sed}$; 15% Al_2O_3.

to 10% sediment with depleted peridotite. This calculation is based on an Os abundance in the peridotite of 2.5 to 3 times that in the subducted rocks (Fig. 3) (*24*). Slightly more sediment (up to 20%) and a higher proportion of the Os in peridotite of 4:1 result in about 6% of subduction component being added to depleted peridotite to produce the most radiogenic Ichinomegata Os compositions. Our inferences about proportions of basalt and sediment are similar to those obtained from analysis of Sr, Nd, Pb, and B isotopes and trace element data in arc lavas from other arcs (*2*). Higher proportions of sediment to basalt (that is, >20% sediment) result in curves that lie to the left of the data fields in Fig. 3. Likewise, lower proportions of Os in peridotite beyond 2:1 to 4:1 do not fit the data. If the average Os abundances for the Simcoe and Ichinomegata peridotite suites are used to represent intrinsic mantle abundances (720 and 894 ppt, respectively), then the Os abundance for the subduction component ranges from 225 to 290 ppt, which is within the uppermost part of the range reported for basalts and ocean sediments (*24*). Peridotites commonly have 1 to 5 parts per billion (ppb) Os (*24*). Therefore, the low concentrations of Os in the xenoliths might result from metasomatism in oxidizing conditions where Os is moderately incompatible (*24*) and where mantle sulfides may not have been as stable as in less oxidizing regimes (*25*).

The Simcoe data are best explained by addition of a component with radiogenic Os and low Al_2O_3 to the depleted mantle (Fig. 4). Aluminum is sparingly soluble in hydrous fluids, including the slab-derived water-rich fluids calculated to be in equilibrium with bark-arc mantle (*3*). The Al_2O_3-Os relations for the Simcoe samples are thus consistent with interaction between a slab-derived hydrous fluid and depleted mantle. Ichinomegata peridotites may have interacted with a slab-derived melt (*4*) or fluids, as the Al_2O_3 values for the radiogenic Os component or components have a range of 0 to 15%.

The Os data suggest that Os is mobile during dehydration or melting of the slab. In mafic layered intrusions, platinum group elements are thought to be redistributed by hydrous and Cl-rich melts and fluids (*26*). The volatility of platinum group elements, and in particular Os, increases as a function of f_{H_2O} and f_{HCl} in magmatic fluids (*27*). A hydrous component, presumably fluids derived from a subducting slab and equilibrated with mantle wedge peridotite, added to a normal mid-ocean ridge basalt–type mantle source, may contain as much as 1.2 weight % Cl (*3*), and possible slab melts are also high in Cl (*4*). Consequently, slab-derived fluids and melts may be particularly effective in transporting Os from slabs into the overlying mantle wedge and arc crust.

REFERENCES AND NOTES

1. J. D. Morris, W. P. Leeman, F. Tera, *Nature* **344**, 31 (1990); T. Plank and C. H. Langmuir, *ibid.* **362**, 739 (1993). For a complete list of references, see R. J. Arculus, *Lithos* **33**, 189 (1994).
2. C. M. H. Edwards, J. D. Morris, M. F. Thirwall, *Nature* **362**, 530 (1993); T. Ishikawa and E. Nakamura, *ibid.* **370**, 205 (1994); J. A. Pearce, P. E. Baker, P. K. Harvey, I. W. Luff, *J. Petrol.* **36**, 1073 (1995).
3. E. Stolper and S. Newman, *Earth Planet. Sci. Lett.* **121**, 293 (1994).
4. P. Schiano *et al.*, *Nature* **377**, 595 (1995).
5. J. W. Morgan and J. F. Lovering, *Earth Planet. Sci. Lett.* **3**, 219 (1967); J. Hertogen, M.-J. Janssens, H. Palme, *Geochim. Cosmochim. Acta* **44**, 2125 (1980); J. W. Morgan, G. A. Wandless, R. K. Petrie, A. J. Irving, *Tectonophysics* **75**, 47 (1981); C.-L. Chou, C. M. Shaw, J. H. Crocket, *J. Geophys. Res.* **88**, A507 (1983); J. M. Luck and C. J. Allegre, *Earth Planet. Sci. Lett.* **107**, 406 (1991); C. E. Martin, *Geochim. Cosmochim. Acta* **55**, 1421 (1991); L. Reisberg, C. J. Allegre, J. M. Luck, *Earth Planet. Sci. Lett.* **105**, 196 (1991).
6. R. J. Walker, R. W. Carlson, S. B. Shirey, F. R. Boyd, *Geochim. Cosmochim. Acta* **53**, 1583 (1989); D. G. Pearson *et al.*, *ibid.* **59**, 959 (1995); D. G. Pearson, R. W. Carlson, S. B. Shirey, F. R. Boyd, P. H. Nixon, *Earth Planet. Sci. Lett.* **134**, 341 (1995).
7. R. W. Carlson and A. J. Irving, *Earth Planet. Sci. Lett.* **126**, 457 (1994).
8. B. K. Esser and K. K. Turekian, *Geochim. Cosmochim. Acta* **52**, 1383 (1988) G. Ravizza, K. K. Turekian, B. J. Hay, *ibid.* **55**, 3741 (1991); G. Ravizza and K. K. Turekian, *Earth Planet. Sci. Lett.* **110**, 1 (1992); G. Ravizza and G. M. McMurtry, *Geochim. Cosmochim. Acta* **57**, 4301 (1993); G. Ravizza, *Earth Planet. Sci. Lett.* **118**, 335 (1993); ______ and B. K. Esser, *Chem. Geol.* **107**, 255 (1993); B. K. Esser and K. K. Turekian, *Geochim. Cosmochim. Acta* **57**, 3093 (1993); B. Peucker-Ehrenbrink, G. Ravizza, A. W. Hoffman, *Earth Planet. Sci. Lett.* **130**, 155 (1995).
9. M. Roy-Barman and C. J. Allegre, *Geochim. Cosmochim. Acta* **58**, 5043 (1994), J. E. Snow and L. Reisberg, *Earth Planet. Sci. Lett.* **133**, 411 (1995).
10. C. E. Martin, B. K. Esser, K. K. Turekian, *Aust. J. Earth Sci.* **38**, 569 (1991).
11. R. J. Walker, L. M. Echeverria, S. B. Shirey, M. F. Horan, *Contrib. Mineral. Petrol.* **107**, 150 (1991).
12. W. J. Pegram and C. J. Allegre, *Earth Planet. Sci. Lett.* **111**, 59 (1992). E. H. Hauri and S. R. Hart, *ibid.* **114**, 353 (1993); L. C. Reisberg *et al.*, *ibid.* **120**, 149 (1993); M. Roy-Barman and C. J. Allegre, *ibid.* **129**, 145 (1995); F. Marcantonio, A. Zindler, T. Elliot, H. Staudigel, *ibid.* **133**, 397 (1995).
13. M. Lidner, D. A. Leich, G. P. Russ, J. M. Bazan, R. J. Borg, *Geochim. Cosmochim. Acta* **53**, 1597 (1989).
14. H. Kuno, in *Ultramafic Related Rocks*, P. J. Wyllie, Ed. (Wiley, New York, 1967), pp. 337–342; E. Takahashi, *Geochim. Cosmochim. Acta* **44**, 1643 (1980); *J. Volcanol. Geotherm Res.* **29**, 355 (1986).
15. D. S. Draper, *J. Geol.* **100**, 766 (1992).
16. A. D. Brandon, R. A. Creaser, S. B. Shirey, *Publicaciones del Instituto Andaluz de Ciencas de la Tierra de Granada* **1**, 8 (1995).
17. K. T. M. Johnson, H. J. B. Dick, N. Shimizu, *J. Geophys. Res.* **95**, 2661 (1990).
18. D. R. Porcelli, R. K. O'Nions, S. J. Galer, A. S. Cohen, D. P. Mattey, *Contrib. Mineral. Petrol.* **110**, 528 (1992).
19. B. J. Wood and D. Virgo, *Geochim. Cosmochim. Acta* **53**, 1277 (1989).
20. A. D. Brandon and D. S. Draper, *ibid.*, in press.
21. B. J. Wood, L. T. Bryndzia, K. E. Johnson, *Science* **248**, 337 (1990); C. Ballhaus, *Contrib. Mineral. Petrol.* **114**, 331 (1993).
22. W. P. Leeman, D. R. Smith, W. Hildreth, Z. Palacz, N. Rodgers, *J. Geophys. Res.* **95**, 19561 (1990).
23. L. Reisberg and J. P. Lorand, *Nature* **376**, 159 (1995).
24. Several assumptions and conditions are involved in the calculations. The Os abundances in peridotites range from 100 ppt to 5 ppb (*5–7, 9, 10*). Abundances lower than 1 ppb are common in mantle xenoliths and in our samples and may result from sulfide loss during entrainment in the host lava or from alteration [J. P. Lorand, *Geochim. Cosmochim. Acta* **54**, 1487 (1990); *Earth Planet. Sci. Lett.* **119**, 627 (1993)], may reflect original heterogeneity at the sample scale (that is, the nugget effect for sulfides) or at larger scales, or may result from oxidizing conditions as suggested here. The Os abundances in basalts and ocean sediments are similar and range from ~10 to 500 ppt (*5, 10–12*). We assume that Os abundances in basalt and ocean sediment are equal for the calculation of the subduction component. We assume that the present-day $^{187}Os/^{188}Os$ is 0.122 for depleted peridotite is at the low end of abyssal peridotite data (*9, 10*), that an initial $^{187}Os/^{188}Os$ for slab basalt is 0.126, and that a present-day $^{187}Os/^{188}Os$ for ocean sediment is 1.023 [data are from (*8*), following (*10*)]. To calculate the present-day $^{187}Os/^{188}Os$ for the hydrous basalt being subducted in the Juan de Fuca (Cascades) and Pacific (Japan) plates, a median $^{187}Re/^{188}Os$ ratio of 240 [mid-ocean ridge basalts and ocean island basalts range from ~20 to >>500 (*10–12*)] is used, and the $^{187}Os/^{188}Os$ ratio is allowed to evolve from 25 Ma (Juan de Fuca) and 175 Ma (Pacific) to the present. This results in present-day $^{187}Os/^{188}Os$ for the Juan de Fuca plate basalt of 0.220 and for the Pacific plate basalt of 0.7945. The proportions of these calculated basalt compositions are mixed with ocean sediment to obtain the $^{187}Os/^{188}Os$ ratio of the subduction component. The Nd abundances and isotopic compositions used for the subduction component are those for mid-ocean ridge basalts [7.3 parts per million (ppm) Nd and $^{143}Nd/^{144}Nd = 0.513150$] and for north Pacific pelagic sediment [average is from D. Ben Othman, W. M. White, J. Patchett, *Earth Planet. Sci. Lett.* **94**, 1 (1989), and is equal to 109.3 ppm Nd and $^{143}Nd/^{144}Nd = 0.512331$]. For the depleted mantle, abyssal peridotite is used and is equal to 0.9 ppm Nd and $^{143}Nd/^{144}Nd = 0.51325$ [see J. E. Snow, S. R. Hart, H. J. B. Dick, *Nature* **371**, 57 (1994)].
25. I. S. E. Carmichael and M. S. Ghiorso, *Earth Planet. Sci. Lett.* **78**, 200 (1986).
26. C. M. Schiffries, *Econ. Geol.* **77**, 1493 (1982); C. G. Ballhaus and E. F. Stumpfl, *Earth Planet. Sci. Lett.* **74**, 56 (1985); *Contrib. Mineral. Petrol.* **94**, 192 (1986); A. E. Boudreau, E. Mathez, I. S. McCallum, *J. Petrol.* **27**, 967 (1986); A. E. Boudreau and I. S. McCallum, *Contrib. Mineral. Petrol.* **102**, 138 (1989).
27. S. A. Wood, *Geochim. Cosmochim. Acta* **51**, 3041 (1987).
28. S. B. Shirey and R. J. Walker, *Anal. Chem.* **34**, 2136 (1995).
29. Sm-Nd isotopic data for handpicked clinopyroxene separates, with procedures for picking, leaching, chemical separation, and mass spectrometry, are reported elsewhere (*7*). Sm and Nd abundances were obtained by isotope dilution. Nd was measured as NdO^+ and corrected to $^{146}NdO/^{144}NdO = 0.72250$ ($^{146}Nd/^{144}Nd = 0.7219$). The reported $^{143}Nd/^{144}Nd$ values are relative to the La Jolla standard of $^{143}Nd/^{144}Nd = 0.511860$ and have precisions of less than ± 0.004% (2σ). Re and Os isotopic data on bulk rock powders were obtained by negative thermal ionization mass spectrometry. Chemical separation and mass spectrometry procedures are reported elsewhere [R. A. Creaser, D. A. Papanastassiou, G. J. Wasserburg, *Geochim. Cosmochim. Acta* **55**, 397 (1991)] (*28*). Re and Os abundances were obtained by isotope dilution. Samples in Table 1 marked with an asterisk were dissolved with aqua regia in Carius tubes at the Department of Terrestrial Magnetism (DTM); the others were dissolved in 120-ml Teflon vessels with successive treatments of concentrated HF, HCl, and H_2SO_4 at the University of Alberta. Both methods result in reproducible abundances and isotopic compositions on peridotite samples (*28*). The reported $^{187}Os/^{188}Os$ values are relative to the Johnson Mathey Os standard of $^{187}Os/^{188}Os = 0.1744$ and have precisions of ±0.3 to 0.8% (2σ).
30. Subcontinental lithospheric mantle Al_2O_3 data are from F. R. Boyd and S. A. Mertzman, in *Magmatic Processes: Physiochemical Principles*, B. O. Mysen, Ed. (Geochemical Society, University Park, PA, 1987), pp. 13–24 (Kaapvaal craton xenoliths). For other locales, Al_2O_3 data are from table 1.2.11.4 in the Basaltic Volcanism Study Project, *Basaltic Volcanism on the Terrestrial*

Planets (Pergamon, New York, 1981), p. 288, and Os isotopes are from T. Meisel and R. J. Walker, *Journal of Conference Abstracts*, 6th V. M. Goldschmidt Conference, Heidelberg, Germany, 1996 (Cambridge Publications, Cambridge, 1996), vol. 1, p. 396. Abyssal peridotite Al_2O_3 data are from J. E. Snow and H. J. B. Dick, *Geochim. Cosmochim. Acta* **59**, 4219 (1995).

31. We thank B. McDonough and F. Frey for Ichinomegata samples and unpublished Al_2O_3 data. Reviews by M. Humayun, L. Reisberg, and three anonymous reviewers and discussion with P. Kelemen were helpful. Supported by Carnegie Foundation and NSF postdoctoral fellowships to A.D.B. and by NSF grants EAR 9204718 and EAR 9506713 to S.B.S. and R.W.C.

5 December 1995; accepted 15 March 1996

Amino Acid Racemization and the Preservation of Ancient DNA

Hendrik N. Poinar, Matthias Höss,* Jeffrey L. Bada, Svante Pääbo

The extent of racemization of aspartic acid, alanine, and leucine provides criteria for assessing whether ancient tissue samples contain endogenous DNA. In samples in which the D/L ratio of aspartic acid exceeds 0.08, ancient DNA sequences could not be retrieved. Paleontological finds from which DNA sequences purportedly millions of years old have been reported show extensive racemization, and the amino acids present are mainly contaminates. An exception is the amino acids in some insects preserved in amber.

The invention of the polymerase chain reaction (*1*) has made it possible to determine DNA sequences from remnants of extinct species and past populations (*2*, *3*). In addition, recent reports have claimed that DNA can be retrieved from paleontological finds that are millions of years old (*4*). However, because only a minority of ancient specimens contain amplifiable ancient DNA (*5*), false positives resulting from minute amounts of contaminating DNA pose a serious threat (*6*, *7*). Although several ways to authenticate ancient DNA have been suggested (*2*, *6*, *8*), the field is in need of techniques that can indicate whether a particular ancient specimen may contain endogenous nucleic acids.

All amino acids used in proteins, with the exception of glycine (Gly), can exist in the form of two optical isomers, the D- and L-enantiomers, of which the L-enantiomer is used exclusively in protein biosynthesis. Once isolated from active metabolic processes, the L-amino acids undergo racemization to produce D-amino acids until eventually the L- and D-enantiomers of a particular amino acid are present in equal amounts. The rate at which racemization takes place differs for each amino acid and is dependent on the presence of water, the temperature, and the chelation of certain metal ions to proteins (*9*). Racemization is thus affected by some of the same factors that affect depurination of DNA, the major hydrolytic reaction responsible for the spontaneous degradation of nucleic acids (*10*). The racemization of aspartic acid (Asp), which has one of the fastest racemization rates, has an activation energy and rate constants over a wide temperature range (at neutral pH) that are similar to those for DNA depurination (*10*, *11*). To test whether the extent of amino acid racemization is a useful indicator of the extent of DNA degradation in ancient specimens, we examined archaeological specimens from which DNA sequences have been retrieved (*12*). In order to ensure as far as possible that the samples used yield genuinely ancient DNA, we limited our analysis to nine cases that fulfill a number of criteria of authenticity (*2*, *6*, *8*) and we excluded human remains because of the inherent difficulty of recognizing contamination from contemporary humans (*2*, *6*, *8*). We also analyzed 17 samples, including some human samples, from which no ancient DNA sequences could be amplified.

No DNA sequences could be retrieved from samples in which the D/L Asp ratio was higher than 0.08 (Table 1), whereas all samples with D/L ratios below 0.08 yielded DNA sequences. Furthermore, there was a rough relation between the extent of Asp racemization and the length of the retrievable DNA sequences (Fig. 1). In samples in which the extent of Asp racemization was similar to that caused by the 6 N HCl hydrolysis procedure (D/L = 0.05), sequences between 140 and 340 base pairs (bp) could be amplified, whereas samples with greater amounts of racemization tended to yield only shorter DNA fragments.

No general correlation was observed between the age of the samples and the retrieval of DNA or the extent of racemization. However, of the nine samples that yielded DNA, seven stemmed from cold environments and four of them have been shown to contain smaller amounts of DNA damage than samples that do not yield amplifiable DNA sequences (*13*). On the basis of the racemization half-lives of Asp reported for bone in various climatic regimes (*9*), the finding that an Asp D/L ratio of about 0.1 is the limit for the retrieval of useful DNA sequences implies that the survival of DNA is limited to a few thousand years in warm regions such as Egypt and to roughly 10^5 years in cold regions. Such temporal limits for DNA retrieval are similar to those predicted from laboratory experiments (*10*). Aspects of amino acid preservation other than racemization do not show any correlation with DNA preservation (*14*).

Because the racemization of Asp is faster than that of other amino acids (*9*, *11*), the extent of racemization of Asp, among the amino acids analyzed here, should be the greatest, followed by alanine (Ala) and leucine (Leu), if all amino acids are of the same age. In contrast, a D/L ratio for Asp that is lower than that for Ala or Leu indicates contamination by more recent amino acids. For the samples from which ancient DNA sequences could be retrieved (Table 1), the extent of racemization of Asp was always greater than that for Ala and Leu, however, no authentic DNA sequences could be retrieved from samples in which the racemization of amino acids did not follow this pattern. Thus, amino acid racemization provides a way to identify the large majority of ancient samples that are not expected to yield any ancient DNA. The usefulness of this technique is enhanced by the fact that samples of only a few milligrams are sufficient for the analysis, and the results can be obtained in only a few days.

Ancient DNA sequences that are purportedly millions of years old have been reported from dinosaur bones, Miocene plant fossils, and amber inclusions (*4*). The D/L Asp ratio in the Utah dinosaur bone

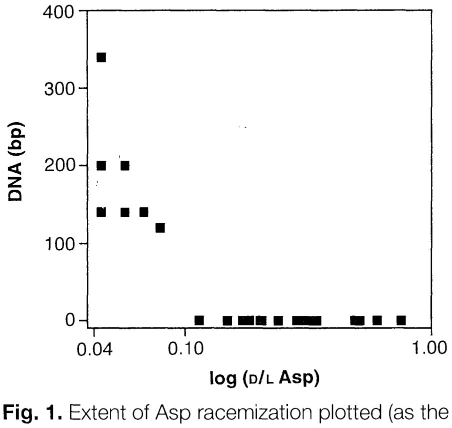

Fig. 1. Extent of Asp racemization plotted (as the logarithm of the D/L ratio of Asp) against the maximum length of DNA amplified (in base pairs).

H. N. Poinar, M. Höss, S. Pääbo, Institute of Zoology, University of Munich, Post Office Box 202136, D-80021 Munich, Germany.
J. L. Bada, Scripps Institution of Oceanography, University of California at San Diego, La Jolla, CA 92093, USA.

*Present address: Clare Hall Laboratories, Imperial Cancer Research Fund, South Mimms, Herts EN6 3LD, UK.